

# Cracking the Code of Hallucination in LVLMs with Vision-aware Head Divergence

Jinghan He<sup>1,2</sup>, Kuan Zhu<sup>1,2</sup>, Haiyun Guo<sup>1,2</sup>, Junfeng Fang<sup>3</sup>, Zhenglin Hua<sup>4</sup>,  
Yuheng Jia<sup>4</sup>, Ming Tang<sup>1</sup>, Tat-Seng Chua<sup>5</sup>, Jinqiao Wang<sup>1,2</sup>

<sup>1</sup>Foundation Model Research Center, Institute of Automation, Chinese Academy of Sciences

<sup>2</sup>School of Artificial Intelligence, University of Chinese Academy of Sciences

<sup>3</sup>University of Science and Technology of China

<sup>4</sup>Southeast University <sup>5</sup>National University of Singapore

hejinghan2022@ia.ac.cn, {kuan.zhu, haiyun.guo, jqwang}@nlpr.ia.ac.cn

## Abstract

Large vision-language models (LVLMs) have made substantial progress in integrating large language models (LLMs) with visual inputs, enabling advanced multimodal reasoning. Despite their success, a persistent challenge is hallucination—where generated text fails to accurately reflect visual content—undermining both accuracy and reliability. Existing methods focus on alignment training or decoding refinements but primarily address symptoms at the generation stage without probing the underlying causes. In this work, we investigate the internal mechanisms driving hallucination in LVLMs, with an emphasis on the multi-head attention module. Specifically, we introduce Vision-aware Head Divergence (VHD), a metric that quantifies the sensitivity of attention head outputs to visual context. Based on this, our findings reveal the presence of vision-aware attention heads that are more attuned to visual information; however, the model’s overreliance on its prior language patterns is closely related to hallucinations. Building on these insights, we propose Vision-aware Head Reinforcement (VHR), a training-free approach to mitigate hallucination by enhancing the role of vision-aware attention heads. Extensive experiments demonstrate that our method achieves superior performance compared to state-of-the-art approaches in mitigating hallucinations, while maintaining high efficiency with negligible additional time overhead.

## 1 Introduction

Large vision-language models (LVLMs) (Dai et al., 2023; Liu et al., 2024b) represent a notable advancement in artificial intelligence by enabling large language models (LLMs) to understand visual inputs. However, LVLMs still face the challenge of hallucination (Rohrbach et al., 2018), where generated text does not accurately correspond to visual content. This misalignment can compromise the accuracy and reliability of LVLMs across a wide

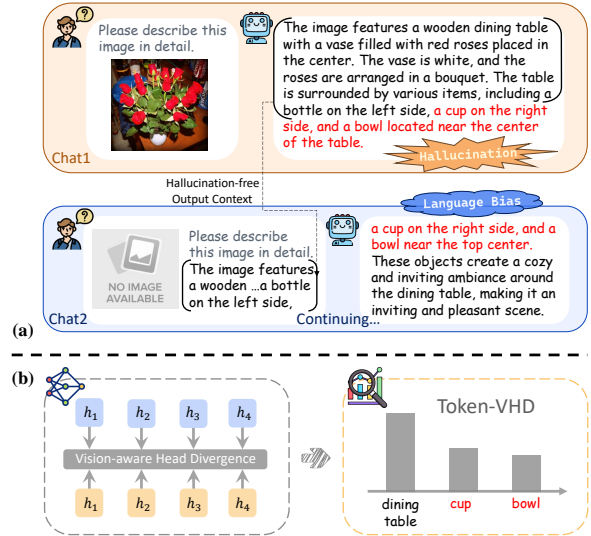


Figure 1: (a) An example indicating the connection between hallucination in LVLMs and language bias. When hallucination occurs (chat 1), we remove the image input and prompt the model to complete the description (chat 2). The output closely resembles the hallucinated content<sup>1</sup>. (b) The proposed VHD metric examines the sensitivity of the attention head outputs to image inputs, revealing their language bias tendency. Hallucinated words generally correspond to lower T-VHD scores.

range of vision and language tasks, limiting their practical applications (You et al., 2024).

To mitigate this issue, several approaches incorporate additional information or models for alignment training (Zhao et al., 2023; Xing et al., 2024) or post-processing (Zhou et al., 2023; Yin et al., 2023), which incur higher training or inference costs. Recently, another line of research focuses on refining decoding strategies, employing methods like contrastive decoding (Leng et al., 2024; Zhu et al., 2024; Kim et al., 2024; Gong et al., 2024) or beam search (Huang et al., 2024) to adjust the logits distribution during inference. However, these approaches merely intervene at the output level

<sup>1</sup>Details on this example are exhibited in Appendix A.

to rectify hallucinations after they occur, without directly targeting and adjusting the internal mechanisms that drive hallucinations. This work aims to fill this research gap.

One of the factors contributing to hallucination in LVLMs is their tendency to prioritize language patterns, which can lead to the generation of fluent but inaccurate content (Liu et al., 2024a). We further investigate this phenomenon and present an example in Figure 1. Specifically, when prompted to continue generating an image description, the model generates highly consistent outputs, irrespective of whether an image is provided. This problem may arise from biased language patterns in the training data, which are incorporated into the model’s parameters (Liu et al., 2024a), causing output to rely more on internal knowledge than image context. Yu et al., 2023 analyzed similar biases in language models and revealed that the multi-head attention module contains both in-context and memory heads. Manipulating these heads can influence whether the output is driven by contextual information or internal knowledge.

Building on previous findings, we are inspired to investigate the relationship between hallucination in LVLMs and the multi-head attention mechanism. To this end, we introduce a novel metric, Vision-aware Head Divergence (VHD), to quantify how the output of each attention head changes when the image context is removed in a generation step of LVLMs. Our analysis reveals that only a few heads show significant sensitivity to the image context, while the majority exhibit minimal variation. Based on this, we aggregate the VHD values from the most prominent attention heads in a generation step, resulting in the Token-VHD (T-VHD) metric. This metric allows us to evaluate the model’s reliance on visual content versus language priors when predicting each token, as illustrated in the bottom-right part of Figure 1. By examining the T-VHD scores, we observe that words and sentences associated with hallucinations generally correspond to lower values, further supporting the role of language bias in hallucination in LVLMs.

Leveraging the insights above, we propose Vision-aware Head Reinforcement (VHR), a training-free approach aimed at enhancing the model’s reliance on visual context rather than language priors. This method proactively mitigates hallucination in LVLMs by first identifying key attention heads based on their VHD scores and then amplifying their contributions during generation.

Theoretical analysis demonstrates that this scaling-up operation effectively re-orientates the output of the multi-head attention module towards the reinforced head component, improving the alignment of the model’s output with visual context. Experiments on established LVLm hallucination benchmarks show that VHR outperforms existing decoding strategies, validating its effectiveness and efficiency in alleviating hallucinations.

Our main contributions can be summarized as follows:

- We propose the VHD metric to probe the attention heads in LVLMs for the language-bias tendency, and the T-VHD metric to analyze the relationship between language-biased generation and hallucination in LVLMs.
- We propose VHR, a training-free method that proactively mitigates hallucinations by adaptively identifying and reinforcing key attention heads during generation.
- Extensive experiments demonstrate that VHR outperforms existing decoding methods on widely-adopted hallucination benchmarks with negligible additional time cost.

## 2 Preliminary

**LVLm generation.** The LVLMs take both image and text as input. The image is encoded into vision tokens using an image encoder and projected to the text embedding space through a connector. These vision tokens  $x_V$  are then combined with tokenized text input  $x_T$  and passed into the LLM component for autoregressive generation:

$$y_t = \arg \max p_\theta(y_t | y_{<t}, x_V, x_T), \quad (1)$$

where  $y_{<t}$  and  $y_t$  denote the earlier and the currently generated text tokens, respectively.

**Multi-head attention.** The multi-head attention mechanism is a core component of transformer models with each attention head performing the self-attention operation among tokens:

$$A_{l,i}(X_{l,i}) = \text{Attention}(X_{l,i}W_{l,i}^Q, X_{l,i}W_{l,i}^K, X_{l,i}W_{l,i}^V),$$

where  $\text{Attention}(Q, K, V) = \text{softmax}\left(\frac{QK^T}{\sqrt{d_k}}\right)V$ .

$$(2)$$

$X_{l,i}$  and  $A_{l,i}$  represent the input and output of the  $h$ -th attention head in the  $l$ -th layer, respectively.  $W^Q$ ,  $W^K$ , and  $W^V$  denote the learned weight matrices for the query, key, and value transformations,

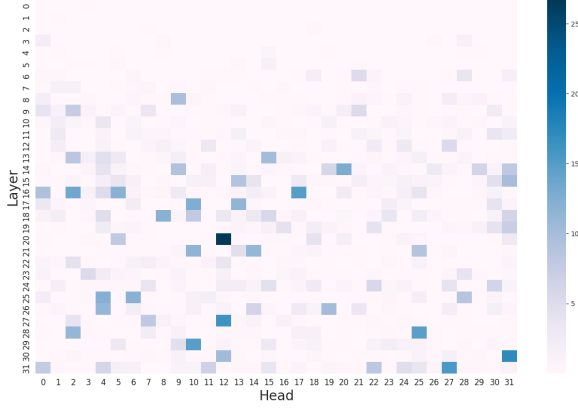


Figure 2: VHD scores of all the attention heads among all layers at one generation step.

respectively.  $d_k$  is the dimension of the query ( $Q$ ) and key ( $K$ ) vectors. The outputs of all the attention heads in the  $l$ -th layer are then concatenated and linearly transformed into the output space of this module:

$$\text{MHA}_l(X_l) = [A_{l,1}(X_{l,1}), \dots, A_{l,n_h}(X_{l,n_h})]W_l^O, \quad (3)$$

where  $n_h$  denotes the number of attention heads in each layer,  $X_l$  is the input to the MHA module in the  $l$ -th layer, and  $W^O$  is the learned weight matrices for the output linear transformation.

**Attention head output during generation.** To more clearly delineate the correspondence between the model’s intermediate outputs and its inputs, we combine Equation 1 and 2 to introduce the notation  $A_{l,i}(y_t|y_{<t}, x_V, x_T)$ . This notation represents the output of the  $i$ -th head in the  $l$ -th layer for generation step  $t$ , given the inputs  $x_V$  and  $x_T$ , and the generation history  $y_{<t}$ .

### 3 Method

#### 3.1 Vision-aware Head Identification

**Vision-aware head divergence (VHD).** Inspired by the presence of in-context and memory heads in the model (Yu et al., 2023), we investigate whether different attention heads exhibit significantly different degrees of sensitivity to visual content. Specifically, we propose the vision-aware head divergence metric, which measures the change in the output of attention head for generation step  $t$  when the image context is removed:

$$\text{VHD}_{l,i} = d(A_{l,i}(y_t|y_{<t}, x_V, x_T), A_{l,i}(y_t|y_{<t}, x_T)), \quad (4)$$

where  $d$  represents the Euclidean distance measure (Tabak, 2014).

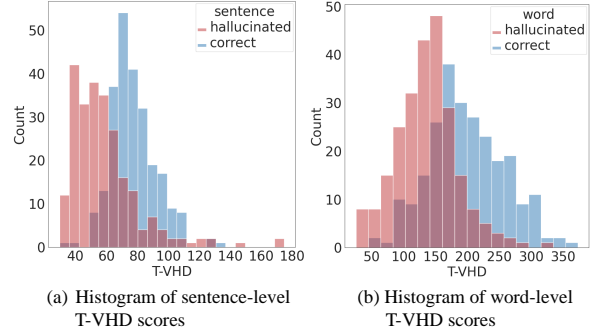


Figure 3: Relationship between T-VHD scores and hallucinations in LVLMs. Sentences and words associated with hallucinations generally correspond to lower T-VHD scores. Best viewed in color.

Figure 2 visualizes the VHD scores for each attention head in the model. Specifically, we prompt LLaVA-1.5 with an image and the instruction "Please describe the image in detail" to generate descriptions, calculating the VHD scores when predicting the first token. The results show that a few attention heads exhibit notably higher VHD scores, while the others show minimal sensitivity. This suggests the presence of vision-aware attention heads that are more attuned to visual information. More examples of VHD scores during the generation process are presented in Appendix E.

**Token-VHD.** Beyond the varying degrees of vision awareness within the model, we further explore whether the VHD scores vary across different token generation steps. To this end, the VHD scores of the most prominent attention heads in each layer of the model are aggregated into the Token-VHD metric:

$$\text{T-VHD} = \sum_l \sum_i \text{topk}_i(\text{VHD}_{l,i}, k). \quad (5)$$

Note that we only consider the top  $k$  VHD scores at each layer to ensure that the large number of insensitive attention heads does not dilute the aggregation metric. Eventually, T-VHD metric serves as an indicator of the model’s reliance on visual information over language priors when predicting a specific token.

Leveraging this metric, we can quantitatively examine the relationship between hallucination in LVLMs and language bias at different levels of granularity, namely at the sentence and word levels. For this purpose, we conduct an experiment on a random sample of 500 images from the CHAIR benchmark (Rohrbach et al., 2018), tracking the T-VHD scores at each generation step. The object-

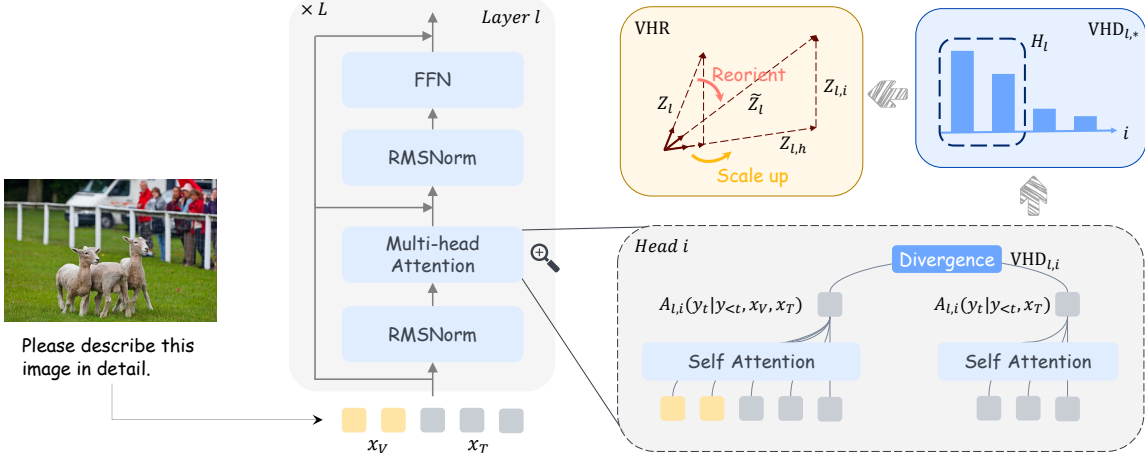


Figure 4: The illustration of the proposed VHD metric and the VHR approach to mitigate hallucinations in LVLm. We select the attention heads that are sensitive to visual information for a given layer based on the VHD metric, *i.e.*  $H_l$ , and then amplify their outputs to reinforce their contributions.

related words in the generated descriptions are classified as hallucinated or correct based on their presence in the annotated object set of the given image, and the sentences are labeled accordingly based on the occurrence of hallucinated words. Figure 3 illustrates the experimental results, highlighting the distributional differences in T-VHD scores between hallucinated and correct data. This further provides statistical evidence that language bias is closely related to hallucinations in LVLms.

### 3.2 Vision-aware Head Reinforcement

Since only a small subset of attention heads within the model are sensitive to visual information, we can amplify their contributions during generation to strengthen the model’s reliance on visual cues and counteract language bias. As discussed in Section 3.1, the VHD metric effectively captures the sensitivity of attention heads to visual information, making it a suitable indicator for selecting key attention heads for reinforcement. However, we observed that some high VHD values stem from a surge in the activation of attention heads upon the removal of visual context, indicating negative vision sensitivity. Amplifying the contributions of such heads would diverge from our objective. Therefore, we propose to zero out these undesired outliers, *i.e.*  $VHD_{l,i} = 0$ , if the following condition satisfies:

$$\begin{cases} VHD_{l,i} > \mu(VHD_{l,*}) + \sigma(VHD_{l,*}), \\ TA_{l,i} > \mu(TA_{l,*}) + \sigma(TA_{l,*}), \end{cases} \quad (6)$$

where  $TA_{l,i} = \|A_{l,i}(y_t|y_{<t}, x_T)\|^2$ .

$\mu$  and  $\sigma$  represent the mean and standard deviation. Next, for the multi-head attention module in a given

layer of the model, we select the first half of the attention heads based on their VHD scores and directly scale up their outputs by a factor of  $\alpha$ :

$$\tilde{A}_{l,i} = \begin{cases} \alpha \cdot A_{l,i}, & \text{if } i \in H_l, \\ A_{l,i}, & \text{otherwise,} \end{cases} \quad (7)$$

where  $H_l = \{i | VHD_{l,i} > \text{median}(VHD_{l,*})\}$ .

**Apply VHR layer by layer.** This specific implementation allows for the selection and reinforcement of attention heads within a single forward pass, as opposed to first selecting the heads in all layers and then reinforcing them in two separate passes. Additionally, when VHR is applied across multiple layers simultaneously, the reinforcement in earlier layers can influence the VHD scores of subsequent layers. The layer-by-layer VHR strategy helps to avoid such inconsistencies, as the previous layers are already reinforced when calculating the VHD scores for a given layer.

**Determine the heads at the first generation step.** Although we can compute the VHD scores and select the key heads at each generation step, reinforcing different heads at different steps may bring negative effects. Specifically, LVLms rely on KV caching to speed up inference, which means that the keys and values of the previous tokens will not be recalculated in subsequent generation steps. Therefore, the key heads should be determined at the beginning of the generation process to ensure consistency in the  $Q$ ,  $K$ , and  $V$  of all tokens in the attention module. Our experimental results show that this approach is sufficient to mitigate hallucinations.

**Comparison with other head identification methods.** Different from existing attention head identification methods in the field of model interpretability (Yu et al., 2023; Li et al., 2024), VHR does not require any annotation and can adaptively detect the key heads for each sample. Furthermore, rather than identifying and reinforcing all key attention heads in the model in two forward passes, VHR ensures computational efficiency and metric consistency by iteratively applying the *select-then-reinforce* approach across the layers. The complete procedure of VHR is provided in Algorithm 1.

### 3.3 Attention Output Reorientation

Scaling up the outputs of certain attention heads within a layer to reinforce its contribution is a straightforward and intuitive operation, and we present a theoretical analysis to substantiate its rationale. Consider the input to the FFN module following the MHA module in layer  $l$ , which can be expressed as follows:

$$\begin{aligned} Z_l &= \text{RMSNorm}(\hat{X}_l + \text{MHA}_l(X_l)) \\ &= \hat{g}_l \cdot \frac{\hat{X}_l + \text{MHA}_l(X_l)}{\|\hat{X}_l + \text{MHA}_l(X_l)\|}, \end{aligned} \quad (8)$$

where  $\hat{g}_l$  is a fixed constant after training, and  $\hat{X}_l$  is the input to the  $l$ -th layer before RMSNorm. Due to the normalization operation, only the direction of the overall output from earlier modules is crucial.

**Proposition 1** *Consider a layer  $l$  within an LVLm, and let  $h$  be the index of the attention head to be reinforced. Let  $\tilde{Z}_l$  be the input to the FFN module obtained with  $\tilde{A}_{l,h} = \alpha \cdot A_{l,h}$  ( $\alpha > 1$ ),  $Z_l$  be original input obtained with  $A_{l,h}$ ,  $Z_{l,h}$  be the pseudo-input obtained with only the  $A_{l,h}$  component. Then it holds that  $\cos(\tilde{Z}_l, Z_{l,h}) > \cos(Z_l, Z_{l,h})$ .*

The proof is detailed in Appendix B. Proposition 1 implies that amplifying the output of a specific head in the MHA module effectively reorients the direction of  $Z_l$  towards the output direction of the reinforced head component. This provides theoretical support for the mechanism underlying the reinforcement of the key attention head. An overview of the proposed VHD metric and the VHR method is presented in Figure 4.

## 4 Experiments

### 4.1 LVLms

We conduct experiments on three of the most representative LVLms, *i.e.* InstructBLIP-7b (Dai

---

### Algorithm 1 VHR

---

**Input** Image  $x_V$ , instruction  $x_T$ , generation step  $t$ , scale factor  $\alpha$ , layers to reinforce  $L_r$

```

1: for layer  $l \in L_r$  do
2:   if  $t = 0$  then
3:     Compute  $\text{VHD}_{l,*}$  ▷ Equation 4
4:     Zero out  $\text{VHD}_{l,i}$  if Equation 6 holds
5:     Select the heads as  $H_l$  ▷ Equation 7
6:   end if
7:   Reinforce the heads in  $H_l$  ▷ Equation 7
8: end for

```

---

et al., 2023), LLaVA-1.5-7b (Liu et al., 2024b), and LLaVA-NeXT-7b (Liu et al., 2024c). LVLms are typically composed of an image encoder, a connector, and an LLM. Specifically, LLaVA-1.5-7b and LLaVA-Next-7b leverage MLP to align the visual and textual embedding space and feed all the image tokens from the image encoder to the LLM. In contrast, InstructBLIP uses Q-Former to reduce the number of image tokens before passing them to the LLM. LLaVA-NeXT differs from LLaVA-1.5 by offering a higher image resolution, allowing it to capture more visual details.

### 4.2 Benchmarks

**CHAIR.** The Caption Hallucination Assessment with Image Relevance (CHAIR) metric (Rohrbach et al., 2018) evaluates object hallucination in image captioning by comparing generated captions with ground truth data. It identifies objects mentioned in captions but absent in images and calculates their proportion to quantify hallucination. Specifically, CHAIR includes two metrics at both caption level ( $\text{CHAIR}_S$ ) and object level ( $\text{CHAIR}_I$ ):

$$\begin{aligned} \text{CHAIR}_S &= \frac{|\{\text{caption w/ hallucinated objects}\}|}{|\{\text{all captions}\}|}, \\ \text{CHAIR}_I &= \frac{|\{\text{hallucinated objects}\}|}{|\{\text{all mentioned objects}\}|}. \end{aligned} \quad (9)$$

We randomly sample 500 images from the COCO 2014 validation set and repeat the experiments for five times with different random seeds. The LVLms are prompted with "Please describe this image in detail." to get the descriptions. We report the average results for each metric along with the standard deviation.

**POPE.** POPE (Li et al., 2023) is a dataset for evaluating object hallucinations by having models answer true or false questions about the presence of

	InstructBLIP			LLaVA-1.5			LLaVA-NeXT		
	CHAIR <sub>S</sub> ↓	CHAIR <sub>I</sub> ↓	Len	CHAIR <sub>S</sub> ↓	CHAIR <sub>I</sub> ↓	Len	CHAIR <sub>S</sub> ↓	CHAIR <sub>I</sub> ↓	Len
Greedy	45.32 $\pm$ 2.24	12.98 $\pm$ 0.76	91.06	49.68 $\pm$ 1.47	14.32 $\pm$ 0.78	83.06	29.08 $\pm$ 2.09	8.08 $\pm$ 0.74	157.06
Beam	48.56 $\pm$ 1.66	13.50 $\pm$ 0.44	94.87	53.84 $\pm$ 2.41	15.60 $\pm$ 0.46	87.47	<u>25.72</u> $\pm$ 2.17	6.92 $\pm$ 0.88	160.64
DoLa	46.00 $\pm$ 1.87	13.00 $\pm$ 0.91	90.75	50.88 $\pm$ 2.34	14.64 $\pm$ 0.90	82.41	28.76 $\pm$ 2.58	8.12 $\pm$ 0.78	155.75
VCD	50.72 $\pm$ 2.44	14.42 $\pm$ 0.99	90.39	51.92 $\pm$ 1.87	15.42 $\pm$ 0.84	83.12	30.80 $\pm$ 2.48	8.72 $\pm$ 0.94	157.72
OPERA	45.76 $\pm$ 2.32	13.06 $\pm$ 0.88	92.46	44.28 $\pm$ 0.95	13.36 $\pm$ 0.47	75.88	-	-	-
CODE	50.76 $\pm$ 2.06	14.12 $\pm$ 0.93	88.57	47.96 $\pm$ 0.80	14.26 $\pm$ 0.57	78.52	27.84 $\pm$ 2.73	7.98 $\pm$ 0.92	151.51
EAH	46.40 $\pm$ 1.15	13.13 $\pm$ 0.60	92.33	<u>38.76</u> $\pm$ 2.47	<u>11.05</u> $\pm$ 0.81	86.28	28.13 $\pm$ 1.13	<b>6.62</b> $\pm$ 0.49	142.75
VHR	<b>38.68</b> $\pm$ 1.70	<b>10.09</b> $\pm$ 1.02	103.29	<b>33.32</b> $\pm$ 1.31	<b>9.71</b> $\pm$ 0.45	81.33	<b>25.00</b> $\pm$ 2.10	<u>6.80</u> $\pm$ 0.58	156.96

Table 1: CHAIR evaluation results on MSCOCO dataset averaged over 5 random splits. The best and second-best results are indicated in **bold** and underlined, respectively. *Len* represents the average length of the generated descriptions.

objects in images. The dataset includes 500 images from MSCOCO (Lin et al., 2014), with each image paired with questions like "Is there a <object> in the image?". The evaluation consists of three splits—random, popular, and adversarial—where objects are sampled in different ways. The evaluation metrics include Accuracy, Precision, Recall, and F1 scores, with the results averaged across all three splits.

**LLaVA-Bench.** LLaVA-Bench (In-the-Wild) (Liu et al., 2024b) is a comprehensive benchmark designed to evaluate the performance of vision-language models on a wide range of challenging tasks. It includes 24 images across diverse domains, such as indoor and outdoor scenes, memes, accompanied by 60 carefully crafted questions covering simple question answering, detailed descriptions, and complex reasoning. Due to the open-ended nature and complexity of the responses, we prompt the GPT-4V model to evaluate the LVLMS’ outputs in terms of both accuracy and detailedness.

### 4.3 Baselines

We compare VHR with the popular training-free methods that do not introduce external information or models: DoLa (Chuang et al., 2023) derives the next-token distribution by contrasting the logits from later and earlier layers. VCD (Leng et al., 2024) contrasts the output distribution generated from the original and distorted image. OPERA (Huang et al., 2024) mitigates over-trust in previous summary tokens in beam-search decoding. CODE (Kim et al., 2024) uses self-generated descriptions as contrast references to improve alignment with the actual visual content. EAH (Zhang et al., 2024) enhances the attention sinks on image tokens in shallow layers. In addition, we also com-

pare the performance of base LVLMS using greedy and beam search decoding.

### 4.4 Implementation Details

We set  $\alpha$  to 2 to strike a balance between effectively correcting hallucinations and minimizing the invasiveness of hidden states manipulation. VHR is applied to the second and last 14 layers for LLaVA series and the second and last 18 layers for InstructBLIP. We faithfully reproduced all baseline methods based on their open-source repositories and set the hyperparameters according to the values reported in the papers. The results of all methods are reported under consistent conditions of base models, prompts, and generation parameters to ensure a fair comparison. Specifically, the `max_new_token` is set to 512, and the number of beams is set to 5 for all methods involving beam search.

### 4.5 Results

**CHAIR.** Table 1 presents the performance of VHR in comparison to all baseline approaches on the CHAIR benchmark. The results for OPERA on LLaVA-NeXT are absent due to its excessive memory requirements. VHR demonstrates robust performance across all three LVLMS, achieving reductions of up to 16.36 in CHAIR<sub>S</sub> and 4.61 in CHAIR<sub>I</sub> on LLaVA-1.5. Notably, with increased image resolution and enhanced model capabilities, LLaVA-NeXT already exhibits a significant reduction in hallucinations compared to other base LVLMS, but VHR continues to exhibit notable effectiveness in mitigating its hallucinations. Moreover, VHR consistently outperforms baseline methods with greater stability, requiring only minor trade-offs in the length or richness of the generated description.

	InstructBLIP F1 Score $\uparrow$	LLaVA-1.5 F1 Score $\uparrow$	LLaVA-NeXT F1 Score $\uparrow$
Greedy	<b>85.36</b>	84.98	<u>88.51</u>
Beam	84.40	85.30	87.97
DoLa	85.21	85.07	88.46
VCD	84.67	84.41	88.11
OPERA	84.41	<u>85.45</u>	-
CODE	84.80	84.63	88.44
EAH	85.18	85.03	84.28
VHR	<u>85.26</u>	<b>85.54</b>	<b>88.66</b>

Table 2: POPE evaluation results averaged over popular, adversarial, and random splits. The best and second-best results are indicated in **bold** and underlined, respectively.

	Accuracy $\uparrow$	Detailedness $\uparrow$
LLaVA-1.5	6.529	6.504
LLaVA-1.5 w/ VHR	<b>6.583</b>	6.496
LLaVA-NeXT	6.492	7.117
LLaVA-NeXT w/ VHR	<b>6.538</b>	7.096

Table 3: LLaVA-Bench (In-the-Wild) evaluation results on the LLaVA series. The results were averaged by prompting the GPT4 to score four times.

**POPE.** As shown in Table 2, VHR outperforms all decoding methods considering all LVLMS. Additionally, VHR continues to yield further improvements with the most advanced models. This suggests that VHR enhances models across various performance levels, positioning it as an efficient and effective training-free decoding strategy.

**LLaVA-Bench.** The GPT-4V evaluation results on LLaVA-Bench are presented in Table 3. These results highlight that VHR can also improve the model’s accuracy on highly diverse and challenging tasks, while preserving a consistent level of detailedness.

## 4.6 Ablation Study

**Necessity of adaptively selecting attention heads for each sample.** Since VHR reinforces different attention heads for each sample, we conduct an ablation study to validate the necessity of this strategy. As shown in Table 4, fixing a set of attention heads identified by one sample for reinforcement across all samples leads to a significant performance drop.

**Layers to Reinforce.** Figure 5 shows the ablation study results on the number of the last few layers for reinforcement. Increasing the number of reinforced layers continuously alleviates hallucinations, with optimal performance reached at the last

	CHAIR <sub>S</sub> $\downarrow$	CHAIR <sub>I</sub> $\downarrow$
InstructBLIP w/ VHR	<b>38.68</b>	<b>10.09</b>
InstructBLIP w/ fixed VHR	45.40	13.57
LLaVA-1.5 w/ VHR	<b>33.32</b>	<b>9.71</b>
LLaVA-1.5 w/ fixed VHR	44.72	13.81
LLaVA-NeXT w/ VHR	<b>25.00</b>	<b>6.80</b>
LLaVA-NeXT w/ fixed VHR	36.96	9.80

Table 4: Ablation study on the necessity of adaptively determining the key heads for each sample.

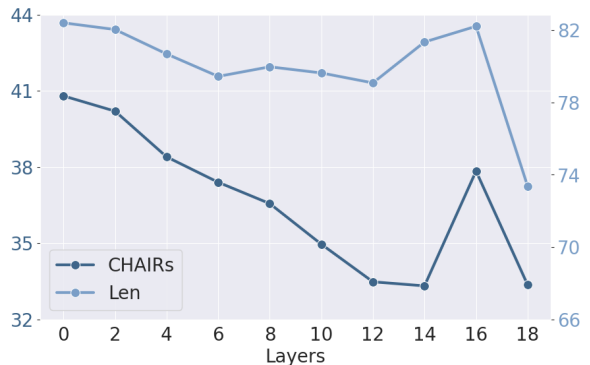


Figure 5: Results of VHR applied across different number of the last few layers.

14 layers. However, further reinforcement degrades the model’s generation quality and fails to effectively mitigate hallucinations. More discussion on the choice of reinforced layers and scale factor can be found in Appendix C and D.

## 4.7 Further Analysis

**Additional Time Analysis.** For the first generation step, VHR requires an additional forward pass, removing the image context to calculate the VHD scores. In subsequent generation steps, only the scaling operation is needed. As a result, the extra computation introduced by VHR is negligible throughout the entire generation process. A detailed inference time comparison between VHR and baseline methods is presented in Figure 6.

**Qualitative Results.** To clearly demonstrate the effect of VHR in reducing hallucinations, we provide a concrete example in Figure 7. Without VHR, the LVM generates content that is absent from the image, such as mentioning people watching the game in the background. This could stem from inherent language bias in the training data. When VHR is applied, the outputs are more accurately aligned with the actual content of the image.

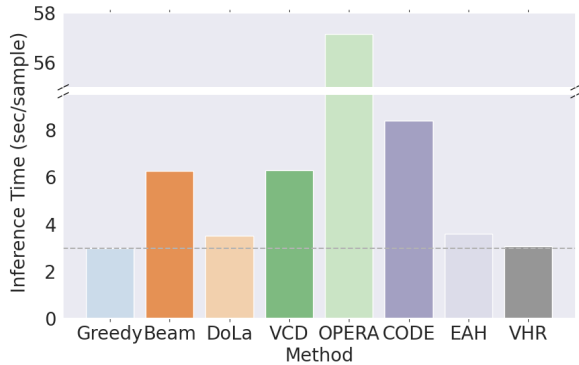


Figure 6: Comparison of inference time for different methods.

## 5 Related Works

### 5.1 Hallucination in LVLMS

Hallucination in LVLMS refers to the inconsistency between the generated text and the image content. This issue arises from multiple factors, including data bias, poor image grounding by vision encoders, misalignment across modalities, *etc* (Liu et al., 2024a). Existing methods to mitigate hallucinations in LVLMS fall into three categories: training alignment (Zhao et al., 2023; Xing et al., 2024), post-processing (Zhou et al., 2023; Yin et al., 2023), and decoding strategies (Leng et al., 2024; Zhu et al., 2024; Huang et al., 2024; Kim et al., 2024; Gong et al., 2024). The first two approaches often rely on external resources or models to improve the performance, whereas VHR relies solely on the model’s internal states without any additional information. Compared with existing decoding strategies, VHR proactively intervenes within the model before hallucinations occur, instead of adjusting the token distributions at the output level. A recent work, EAH(Zhang et al., 2024), also targets the attention mechanism to reduce hallucinations but focuses on the attention sink phenomenon. In contrast, VHR reduces language bias in LVLMS by exploiting cross-modal contrast and directly re-adjusting the attention head contributions across multiple layers. The underlying motivations and methodologies of the two works are different.

### 5.2 Language Bias in LVLMS

Language bias refers to the tendency of models to prioritize language patterns or prior knowledge over visual context. This issue has a long-standing research history predating the emergence of LVLMS and was studied through methods like balanced multimodal training (Goyal et al., 2017)

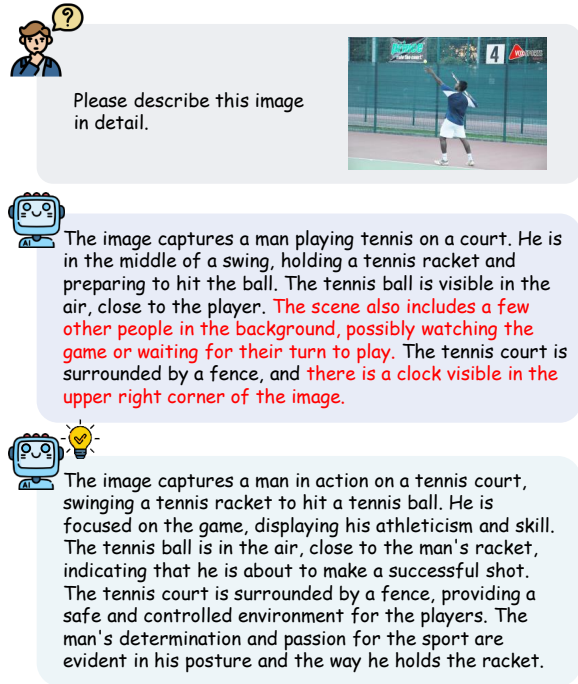


Figure 7: An example of VHR eliminating the hallucinated content.

and causal inference(Niu et al., 2021). With the advent of LVLMS, language bias became an even more pressing concern, as these models are often pre-trained on vast amounts of text, further exacerbating the potential for language overfitting. Some existing methods address this issue by employing contrastive decoding techniques (Leng et al., 2024; Zhu et al., 2024). However, these methods directly manipulate the output logits, which introduces instability in the generation process and lacks an analysis of hallucination and the internal states of the model. Our approach presents a new solution beyond contrast decoding and serves as a complement to this gap.

## 6 Conclusion

This work explores the link between hallucination in LVLMS and the multi-head attention module. We introduce the VHD metric to measure the sensitivity of the attention head outputs to visual context and show that language bias may contribute to hallucination in LVLMS. Based on these insights, we propose VHR, a training-free method that enhances the role of vision-aware attention heads to mitigate hallucinations. Extensive experiments demonstrate that VHR outperforms existing methods, improving model alignment with visual information.



## Limitations

Our analysis and mitigation strategy primarily focuses on the multi-head attention mechanism of LVLMs. While this is a critical component influencing hallucinations, there may be other architectural factors—such as those in the vision encoder and the FFN module in the LLMs—that contribute to hallucinations but were not directly addressed in this study. Future work could focus on more comprehensive interventions that span the entire model, going beyond attention head manipulation.

## References

- Liang Chen, Haozhe Zhao, Tianyu Liu, Shuai Bai, Junyang Lin, Chang Zhou, and Baobao Chang. 2025. An image is worth 1/2 tokens after layer 2: Plug-and-play inference acceleration for large vision-language models. In *European Conference on Computer Vision*, pages 19–35. Springer.
- Yung-Sung Chuang, Yujia Xie, Hongyin Luo, Yoon Kim, James Glass, and Pengcheng He. 2023. Dola: Decoding by contrasting layers improves factuality in large language models. *arXiv preprint arXiv:2309.03883*.
- Wenliang Dai, Junnan Li, Dongxu Li, Anthony Meng Huat Tiong, Junqi Zhao, Weisheng Wang, Boyang Li, Pascale Fung, and Steven Hoi. 2023. *Instructblip: Towards general-purpose vision-language models with instruction tuning*. Preprint, arXiv:2305.06500.
- Xuan Gong, Tianshi Ming, Xinpeng Wang, and Zhihua Wei. 2024. Damro: Dive into the attention mechanism of lvlm to reduce object hallucination. *arXiv preprint arXiv:2410.04514*.
- Yash Goyal, Tejas Khot, Douglas Summers-Stay, Dhruv Batra, and Devi Parikh. 2017. Making the v in vqa matter: Elevating the role of image understanding in visual question answering. In *Proceedings of the IEEE conference on computer vision and pattern recognition*, pages 6904–6913.
- Qidong Huang, Xiaoyi Dong, Pan Zhang, Bin Wang, Conghui He, Jiaqi Wang, Dahua Lin, Weiming Zhang, and Nenghai Yu. 2024. Opera: Alleviating hallucination in multi-modal large language models via over-trust penalty and retrospection-allocation. In *Proceedings of the IEEE/CVF Conference on Computer Vision and Pattern Recognition*, pages 13418–13427.
- Junho Kim, Hyunjun Kim, Yeonju Kim, and Yong Man Ro. 2024. Code: Contrasting self-generated description to combat hallucination in large multi-modal models. *arXiv preprint arXiv:2406.01920*.
- Sicong Leng, Hang Zhang, Guanzheng Chen, Xin Li, Shijian Lu, Chunyan Miao, and Lidong Bing. 2024. Mitigating object hallucinations in large vision-language models through visual contrastive decoding. In *Proceedings of the IEEE/CVF Conference on Computer Vision and Pattern Recognition*, pages 13872–13882.
- Kenneth Li, Oam Patel, Fernanda Viégas, Hanspeter Pfister, and Martin Wattenberg. 2024. Inference-time intervention: Eliciting truthful answers from a language model. *Advances in Neural Information Processing Systems*, 36.
- Yifan Li, Yifan Du, Kun Zhou, Jinpeng Wang, Wayne Xin Zhao, and Ji-Rong Wen. 2023. Evaluating object hallucination in large vision-language models. *arXiv preprint arXiv:2305.10355*.
- Tsung-Yi Lin, Michael Maire, Serge Belongie, James Hays, Pietro Perona, Deva Ramanan, Piotr Dollár, and C Lawrence Zitnick. 2014. Microsoft coco: Common objects in context. In *Computer Vision—ECCV 2014: 13th European Conference, Zurich, Switzerland, September 6-12, 2014, Proceedings, Part V 13*, pages 740–755. Springer.
- Hanchao Liu, Wenyuan Xue, Yifei Chen, Dapeng Chen, Xiutian Zhao, Ke Wang, Liping Hou, Rongjun Li, and Wei Peng. 2024a. A survey on hallucination in large vision-language models. *arXiv preprint arXiv:2402.00253*.
- Haotian Liu, Chunyuan Li, Yuheng Li, and Yong Jae Lee. 2024b. Improved baselines with visual instruction tuning. In *Proceedings of the IEEE/CVF Conference on Computer Vision and Pattern Recognition*, pages 26296–26306.
- Haotian Liu, Chunyuan Li, Yuheng Li, Bo Li, Yuanhan Zhang, Sheng Shen, and Yong Jae Lee. 2024c. *Llava-next: Improved reasoning, ocr, and world knowledge*.
- Yulei Niu, Kaihua Tang, Hanwang Zhang, Zhiwu Lu, Xian-Sheng Hua, and Ji-Rong Wen. 2021. Counterfactual vqa: A cause-effect look at language bias. In *Proceedings of the IEEE/CVF conference on computer vision and pattern recognition*, pages 12700–12710.
- Anna Rohrbach, Lisa Anne Hendricks, Kaylee Burns, Trevor Darrell, and Kate Saenko. 2018. Object hallucination in image captioning. *arXiv preprint arXiv:1809.02156*.
- John Tabak. 2014. *Geometry: the language of space and form*. Infobase Publishing.
- Shangyu Xing, Fei Zhao, Zhen Wu, Tuo An, Weihao Chen, Chunhui Li, Jianbing Zhang, and Xinyu Dai. 2024. Efuf: Efficient fine-grained unlearning framework for mitigating hallucinations in multimodal large language models. *arXiv preprint arXiv:2402.09801*.

Shukang Yin, Chaoyou Fu, Sirui Zhao, Tong Xu, Hao Wang, Dianbo Sui, Yunhang Shen, Ke Li, Xing Sun, and Enhong Chen. 2023. Woodpecker: Hallucination correction for multimodal large language models. *arXiv preprint arXiv:2310.16045*.

Junwei You, Haotian Shi, Zhuoyu Jiang, Zilin Huang, Rui Gan, Keshu Wu, Xi Cheng, Xiaopeng Li, and Bin Ran. 2024. V2x-vlm: End-to-end v2x cooperative autonomous driving through large vision-language models. *arXiv preprint arXiv:2408.09251*.

Qinan Yu, Jack Merullo, and Ellie Pavlick. 2023. Characterizing mechanisms for factual recall in language models. *arXiv preprint arXiv:2310.15910*.

Xiaofeng Zhang, Yihao Quan, Chaochen Gu, Chen Shen, Xiaosong Yuan, Shaotian Yan, Hao Cheng, Kaijie Wu, and Jieping Ye. 2024. Seeing clearly by layer two: Enhancing attention heads to alleviate hallucination in vlms. *arXiv preprint arXiv:2411.09968*.

Zhiyuan Zhao, Bin Wang, Linke Ouyang, Xiaoyi Dong, Jiaqi Wang, and Conghui He. 2023. Beyond hallucinations: Enhancing vlms through hallucination-aware direct preference optimization. *arXiv preprint arXiv:2311.16839*.

Yiyang Zhou, Chenhang Cui, Jaehong Yoon, Linjun Zhang, Zhun Deng, Chelsea Finn, Mohit Bansal, and Huaxiu Yao. 2023. Analyzing and mitigating object hallucination in large vision-language models. *arXiv preprint arXiv:2310.00754*.

Lanyun Zhu, Deyi Ji, Tianrun Chen, Peng Xu, Jieping Ye, and Jun Liu. 2024. Ibd: Alleviating hallucinations in large vision-language models via image-biased decoding. *arXiv preprint arXiv:2402.18476*.

## A An Example of the Language Bias Phenomenon

Figure 8 presents the details on the example that reflect language bias. Specifically, we first prompted the LVLm to describe the image content, resulting in a complete image description. We observed that the latter part of this description includes hallucinated content. To explore the connection between this phenomenon and language bias, we removed the image input and fed the model with the original prompt concatenated with the hallucination-free part of text generated by the LVLm. This allowed us to observe how the model would continue the text based solely on its internal knowledge. We found that the continuation closely resembled the hallucinated content. This particular example effectively demonstrates the connection between language bias and hallucination in LVLms.

In the lower part of Figure 8, we visualize the T-VHD scores for each word generated by the

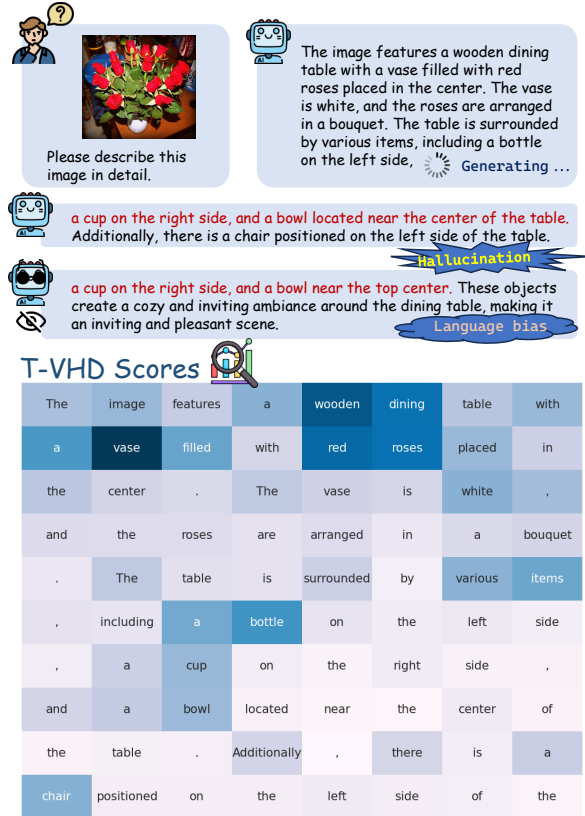


Figure 8: An example indicating the connection between hallucination in LVLms and language bias. The proposed T-VHD metric can reflect the model’s reliance on visual content versus language priors in generating each token.

LVLm in the image description of this example. The color intensity of the words corresponds to their T-VHD scores, with darker colors indicating higher scores. From the results, we observe that words within fixed phrases (e.g. surrounded by, on the right/left side) generally exhibit lower T-VHD scores, while object terms introduced for the first time in the description (e.g. wooden dining table, vase, red roses) tend to show higher T-VHD scores. Additionally, among all the object terms, words corresponding to hallucinations (e.g., cup, bowl and chair) generally display lower T-VHD scores. This example clearly illustrates how the proposed T-VHD metric captures the model’s dependence on visual content as opposed to language prior when generating each token.

## B Attention Output Reorientation

**Proposition 1** Consider a layer  $l$  within an LVLm, and let  $h$  be the index of the attention head to be reinforced. Let  $\tilde{Z}_l$  be the input to the FFN module obtained with  $\tilde{A}_{l,h} = \alpha \cdot A_{l,h}$  ( $\alpha > 1$ ),  $Z_l$  be orig-

inal input obtained with  $A_{l,h}$ ,  $Z_{l,h}$  be the pseudo-input obtained with only the  $A_{l,h}$  component. Then it holds that  $\cos(\tilde{Z}_l, Z_{l,h}) > \cos(Z_l, Z_{l,h})$ .

*Proof.* By partitioning the projection matrix  $W_l^O$ , we can further express the output of the MHA as the sum of the contributions from each attention head:

$$\begin{aligned} \text{MHA}_l(X_l) &= [A_{l,1}(X_{l,1}), \dots, A_{l,n_h}(X_{l,n_h})]W_l^O \\ &= A_{l,1}(X_{l,1})W_{l,1}^O + \dots + A_{l,n_h}(X_{l,n_h})W_{l,n_h}^O. \end{aligned} \quad (10)$$

To simplify the notation, we define  $x$  and  $y$  as follows:

$$\begin{aligned} x &= \hat{X}_l + \text{MHA}_l(X_l), \\ y &= A_{l,h}(X_{l,h})W_{l,h}^O. \end{aligned} \quad (11)$$

We then substitute  $x$  and  $y$  for the variables in Equation 8 to derive  $Z_l, \tilde{Z}_l, Z_{l,h}$ :

$$\begin{aligned} Z_l &= \hat{g}_t \frac{x}{\|x\|}, \\ \tilde{Z}_l &= \hat{g}_t \frac{x + (\alpha - 1)y}{\|x + (\alpha - 1)y\|}, \\ Z_{l,h} &= \hat{g}_t \frac{y}{\|y\|}. \end{aligned} \quad (12)$$

Lastly, we prove that  $\cos(\tilde{Z}_l, Z_{l,h})$  is greater than  $\cos(Z_l, Z_{l,h})$ :

$$\begin{aligned} &\cos(\tilde{Z}_l, Z_{l,h}) - \cos(Z_l, Z_{l,h}) \\ &= \frac{\langle x + (\alpha - 1)y, y \rangle}{\|x + (\alpha - 1)y\| \|y\|} - \frac{\langle x, y \rangle}{\|x\| \|y\|} \\ &= \frac{\langle x + (\alpha - 1)y, (\alpha - 1)y \rangle}{\|x + (\alpha - 1)y\| \|(\alpha - 1)y\|} - \frac{\langle x, (\alpha - 1)y \rangle}{\|x\| \|(\alpha - 1)y\|} \\ &= \frac{\langle x, \hat{y} \rangle + \|\hat{y}\|^2}{\|x + \hat{y}\| \|\hat{y}\|} - \frac{\langle x, \hat{y} \rangle}{\|x\| \|\hat{y}\|} \\ &> \frac{-\|x\| + \|\hat{y}\|}{\|x + \hat{y}\|} + 1 \\ &= \frac{\|x + \hat{y}\| + \|\hat{y}\| - \|x\|}{\|x + \hat{y}\|} \\ &> 0, \end{aligned} \quad (13)$$

which concludes the proof.

## C Choice of Reinforced Layers

Since Chen et al., 2025 and Zhang et al., 2024 have highlighted the unique role of the second layer in integrating visual information through attention map analysis, we include this layer for VHR and further

	CHAIR <sub>S</sub> ↓	CHAIR <sub>I</sub> ↓
LLaVA-1.5	49.68	14.32
w/ VHR on layer1	40.80	12.00
w/ VHR on last 14 layers	41.96	12.56
w/ VHR on both	<b>33.32</b>	<b>9.71</b>

Table 5: Ablation study on the reinforced layers.

	CHAIR <sub>S</sub> ↓	CHAIR <sub>I</sub> ↓	Len
LLaVA-1.5	49.68	14.32	83.06
w/ VHR $\alpha = 0.2$	63.28	21.04	86.42
w/ VHR $\alpha = 0.5$	55.80	17.32	84.47
w/ VHR $\alpha = 2$	33.32	9.71	81.33
w/ VHR $\alpha = 3$	27.04	8.68	88.31
w/ VHR $\alpha = 4$	3.64	2.01	144.54

Table 6: Ablation study on the scale factor.

validated its significance in mitigating hallucinations. Table 5 presents the results of ablation experiments conducted on this layer and the last few layers on LLaVA-1.5. The results show that enhancing layer1 and the deeper layers both significantly alleviate hallucinations, with the combination of both yielding even better results. This suggests that VHR in the model’s shallow and deep layers alleviates hallucinations through distinct mechanisms. We leave further analysis of the specific mechanisms at each layer of LVLMS for future work.

## D Choice of Scale Factor

Table 6 shows the results of ablation experiments on the scale factor  $\alpha$  in VHR. When  $\alpha$  is set to 2 or 3, hallucinations are effectively alleviated. However, as  $\alpha$  increases to 4, excessive intervention disrupts the model’s behavior, causing anomalies in the hallucination metric. Conversely, when  $\alpha < 1$ , which weakens the contribution of attention heads sensitive to visual information, hallucinations become significantly more pronounced. This further confirms the crucial role of the attention heads identified based on the VHD scores in mitigating hallucinations in LVLMS.

## E Examples of VHD Scores

As shown in Figure 10, the first row presents the VHD scores during the first generation step across different samples, while the second row shows the VHD scores for different object terms generated within the same sample. It can be observed that VHD scores vary across different samples and generation steps; however, significant differences be-

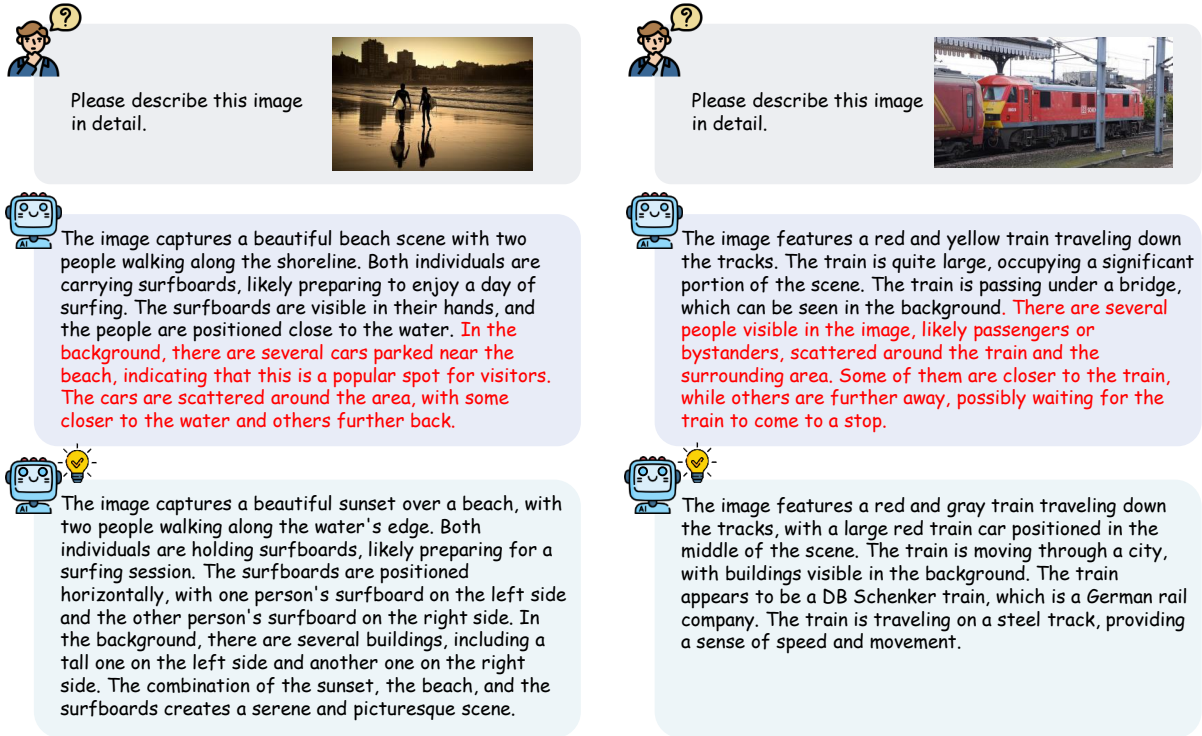


Figure 9: More examples of VHR eliminating the hallucinated content.

tween the VHD scores of the attention heads within the model are consistently present.

## F More Qualitative Results

As shown in Figure 9, we present more examples that illustrate the effect of VHR in eliminating hallucinated objects. After incorporating VHR, the descriptions generated by the LVLMs faithfully align with the content of the images, while preserving the richness of the descriptions.

## G Details on the GPT-4V Evaluation

To evaluate the performance of the LVLMs on LLavaBench, we employ GPT-4o-mini for scoring. For each sample, we follow the template in Table 7 as outlined in (Gong et al., 2024) and provide GPT-4o-mini with the original image, the output from the LVLM and the VHR improved LVLM. The evaluation focuses on the accuracy and detailedness of the model's output, particularly in reducing hallucinations in the VHR-improved model compared to the baseline. During the evaluation, we observed that GPT generally favors the former response compared to the latter one, so we swapped the outputs and repeated the evaluation four times to obtain the averaged results.

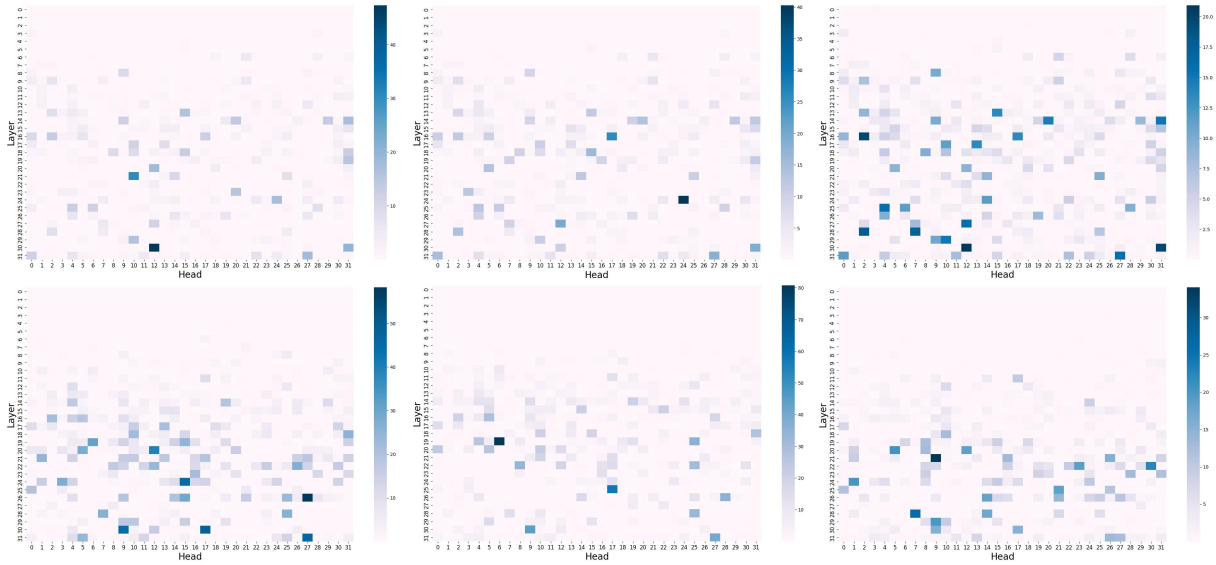


Figure 10: More examples of the VHD scores during different generation steps of different samples.

---

### GPT-4V Prompt

You are required to score the performance of two AI assistants in describing a given image. You should pay extra attention to the hallucination, which refers to the part of descriptions that are inconsistent with the image content, such as claiming the existence of something not present in the image or describing incorrectly in terms of the counts, positions, or colors of objects in the image. Please rate the responses of the assistants on a scale of 1 to 10, where a higher score indicates better performance, according to the following criteria:

- 1: Accuracy: whether the response is accurate with respect to the image content. Responses with fewer hallucinations should be given higher scores.
- 2: Detailedness: whether the response is rich in necessary details. Note that hallucinated descriptions should not count as necessary details.

Please output the scores for each criterion, containing only two values indicating the scores for Assistant 1 and 2, respectively. The two scores are separated by a space. Following the scores, please provide an explanation of your evaluation, avoiding any potential bias and ensuring that the order in which the responses were presented does not affect your judgment.

[Assistant 1]  
 {}  
 [End of Assistant 1]

[Assistant 2]  
 {}  
 [End of Assistant 2]

Output format:  
 Accuracy:  
 Reason:  
 Detailedness:  
 Reason:

---

Table 7: The prompt used for GPT-4V evaluation.